Improving gas tomography with mobile robots: An evaluation of sensing geometries in complex environments

Conference Paper · May 2017

DOI: 10.1109/ISOEN.2017.7968895

CITATIONS
4

READS
43

5 authors, including:

Muhammad Asif Arain
Örebro University
10 PUBLICATIONS **83** CITATIONS
SEE PROFILE

Han Fan
Chalmers University of Technology
16 PUBLICATIONS **220** CITATIONS
SEE PROFILE

Victor Hernandez Bennetts
Örebro University
54 PUBLICATIONS **857** CITATIONS
SEE PROFILE

Achim J. Lilienthal
Örebro University
451 PUBLICATIONS **7,670** CITATIONS
SEE PROFILE

Some of the authors of this publication are also working on these related projects:

Cognitive load and compensatory movements in learning a multi-function prosthetic hand View project

Action and Intention Recognition in Human Interaction with Autonomous Systems (AIR) View project

Improving Gas Tomography with Mobile Robots: An Evaluation of Sensing Geometries in Complex Environments

Muhammad Asif Arain, Han Fan, Victor Hernandez Bennetts, Erik Schaffernicht, and Achim J. Lilienthal
Mobile Robotics & Olfaction Lab, Center for Applied Autonomous Sensor Systems (AASS), Örebro University, Sweden

***Abstract*—An accurate model of gas emissions is of high importance in several real-world applications related to monitoring and surveillance. Gas tomography is a non-intrusive optical method to estimate the spatial distribution of gas concentrations using remote sensors. The choice of sensing geometry, which is the arrangement of sensing positions to perform gas tomography, directly affects the reconstruction quality of the obtained gas distribution maps. In this paper, we present an investigation of criteria that allow to determine suitable sensing geometries for gas tomography. We consider an actuated remote gas sensor installed on a mobile robot, and evaluated a large number of sensing configurations. Experiments in complex settings were conducted using a state-of-the-art CFD-based filament gas dispersal simulator. Our quantitative comparison yields preferred sensing geometries for sensor planning, which allows to better reconstruct gas distributions.**

I. Introduction

Fugitive greenhouse gases, such as methane, are major concern due to their ecological impact, safety hazards, and economical losses. Gas distribution maps that show the spatial distribution of gas concentrations can be used to locate fugitive emissions. In this context, remote gas sensors offer favorable properties to measure gas concentrations in large environments. An example of a remote gas sensing principle is the Tunable Diode Laser Absorption Spectroscopy (TDLAS), which is highly selective and sensitive to its target gases, and provides high operational stability. These sensors report spatially unresolved integral concentrations along the line-of-sight, see Fig. 1(a).

Computer Tomography of Gases (CTG) is a technique used to estimate the spatial distribution of gas concentrations from integral measurements. A typical CTG setup consists of stationary remote sensors and reflectors. A reconstruction algorithm is thus used to estimate the spatial distribution of the concentrations. CTG can be performed by mobile robots using a technique known as Robot Assisted Gas Tomography (RAGT) [1]. A robot equipped with a TDLAS sensor does not require a dedicated reflector, as the floor or any reflective surface in the environment can be used without a significant loss of accuracy. The robot can collect measurements at different locations and, moreover, it allows for adaptive sensor placement with the goal to improve e.g. map quality.

A first step in order to make the problem of finding optimal sensing positions tractable is to define a sensing configuration, assuming a mobile, actuated remote sensor. Fig. 1(b) shows the sensing configuration in this paper, which consists of collecting integral measurements within a circular sector (r, ϕ)

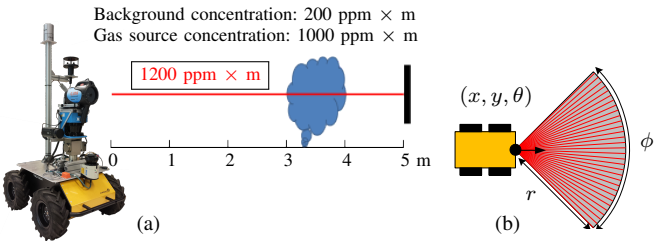

Fig. 1: (a) A TDLAS equipped robot. (b) A RAGT sensing action.

by measuring along s equally spaced beams of length r inside the field of view ϕ at pose (x, y, θ).

The set of all sensing configurations to perform reconstruction is a sensing geometry. Besides the choice of the sensor technology and the reconstruction algorithm, the sensing geometry is of utmost importance for the reconstruction quality [2], [3]. In this paper, we address the question which criteria allow to determine sensing geometries for gas tomography that enhance the reconstruction quality, i.e. on average lead to more truthful gas distribution maps. A first evaluation of sensing geometries, and a sensor planning algorithm for RAGT that chooses the sensing configurations accordingly was published in [3]. However, the evaluation was performed only for limited test cases, where time-invariant, simplified Gaussian-shaped gas distributions were considered in an obstacle-free environment. Moreover, different wind flow conditions were not simulated. In this paper, we address these shortcomings.

Since it is difficult to fully observe gas dispersion in real-world experiments, it is not possible to compare true distributions with their reconstructions. To overcome this limitation, we use a simulation setup that provides ground truth. The contributions of this paper result from extensions of our previous work in the following way: first, we simulate gas dispersion with a state-of-the-art Computational Fluid Dynamics (CFD) based simulator [4], which simulates filament-based gas dispersion in obstacle populated environments instead of time-constant simplified Gaussian plumes; second, a large set of sensing geometries is used to collect remote gas sensor measurements, which are then used to reconstruct the gas distributions. Finally, we compare the obtained gas distribution maps in terms of their reconstruction quality, which we evaluate in two different ways computing (1) the global error of the spatial reconstruction, and (2) the divergence of the probability density function (PDF) of the ground truth and the reconstruction map. In addition, we discuss a possible application of our results for the placement of sensing configurations (i.e. sensor planning) for RAGT.

II. Simulation Setup

We used a CFD based gas dispersion simulator, originally introduced in [4], and recorded 3D gas dispersion snapshots at different time intervals for different, realistic environments and different wind speeds, as well as for different magnitudes of gas source concentrations. In order to avoid the complexities of a full 3D evaluation, all the gas concentrations along the 3rd dimension were integrated and the evaluation was carried out in 2D. 2D reconstructions are common in applications where gas dispersion is interesting, for example, at surface levels only. For each sensing geometry integral measurements were computed and the reconstruction algorithm in [1] was applied to the measurements to obtain gas distribution maps. We then compared the true gas distributions from the CFD-based simulator, and their corresponding reconstructions.

The true gas distributions are given as maps of 100×100 Cartesian grid cells (cell size = 1m). In gas tomography, spatial resolutions is commonly set in the order of meters. The gas sources with different release rates and concentrations up to 5000 ppm distributed over the simulated area, are placed in the middle of the map. The investigated sensing configurations were located on a concentric circle with a radius of 15 cells, orientated towards the gas source. Each sensing configuration was placed in a systematic way, by setting the sensing parameters $r = 30$ cells, $\phi = 90°$, and $s = 90$.

We used sensing geometries that contain $\mathbf{g}_c = [2, 3, 4, 5]$ configurations. For each $\mathbf{g}_c$, the first configuration c_1 is placed on a circle with an incremental step of 10°, starting from 0° (total 36 positions). The remaining configurations $c_2 ... c_n$ are placed with pair-wise equal cross angles $\theta_\times$ in anti-clock wise direction to c_1, and with an incremental step of 2.5° (144 positions), see Fig. 2(a). A maximum of 5184 sensing geometries was thus evaluated for each element in $\mathbf{g}_c$ in one out of 19 test cases. In 8 of those cases the gas distribution was sampled at the same time (corresponding to several remote gas sensors measuring simultaneously) while in 11 test cases the simulated gas distribution was sampled at subsequent times (corresponding to a single robot carrying out RAGT). In the 8 simultaneous sampling cases, gas concentration measurements are collected from an averaged distribution generated at time instances $t_0 ... t_n$. In the subsequent sampling cases, the measurements were collected by executing subsequent sensing configuration at a particular time instance. In both cases, the comparison of the reconstruction is performed against the true gas concentration distributions, averaged over the whole simulation time. Fig. 2(b)-2(e) shows four example test cases. Notice the effect of the wind flow and obstacles in the true gas concentration distributions.

III. Evaluation

In our application of emission monitoring, a *good* reconstruction is one that not only represents the true gas concentration magnitudes as truthfully as possible but also accurately captures the spatial distribution of the gas concentrations. The selected sensing geometry affects the reconstruction quality in the following ways: (1) the number of sensing configurations

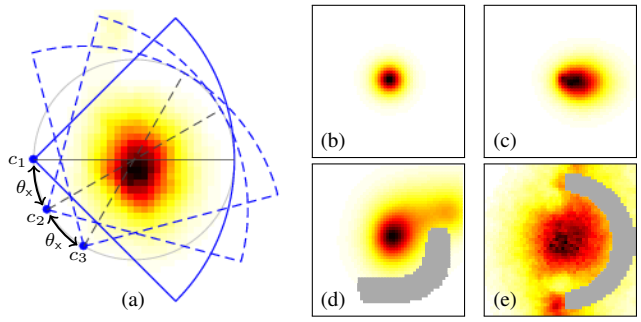

Fig. 2: (a) An instance of $\mathbf{g}_c = 3$, where c_1, c_2, and c_3 are placed with pairwise cross angles $\theta_\times$ on a concentric circle to the gas source. (b)-(e) are selected test cases with different wind flow and obstacles.

in the geometry, (2) the cross angles between the configurations, and (3) sensing parameters such as (r, ϕ, s), which are assumed to be fixed and not evaluated here. We are interested in finding the minimum number of sensing configurations ($\mathbf{g}_c$) and the corresponding cross angles for the best reconstructions.

For the quantitative evaluation of sensing geometries, we used Nearness [2] and Jensen-Shannon divergence (JS-div) [5]. Nearness represents the global reconstruction error. In other words, the error in the concentration values in the Cartesian space. It is defined as

$$\text{Nearness} = \sqrt{\sum_{i=1}^{n} (\widehat{c}_i - c_i)^2 \Big/ \sum_{i=1}^{n} (\widehat{c}_i - \overline{c})^2}$$

where $\widehat{c}_i$ and c_i are the true and the reconstructed concentrations of the ith cell, and $\overline{c}$ is the average true concentration. JS-div computes the divergence between the PDFs of the true gas concentrations (P) and the reconstructed gas distribution (Q). It is a symmetrized version of the Kullback-Leibler divergence $D_{KL}(P \parallel Q)$, and is defined as

$$D_{JS}(P \parallel Q) = 1/2\, D_{KL}(P \parallel M) + 1/2\, D_{KL}(Q \parallel M)$$

where $M = 1/2\,(P + Q)$.

Evaluation of the number of configurations: The averaged results for the best 20 reconstructions of all $\mathbf{g}_c$ are shown in Fig. 3. It can be noticed that the error reduction in Nearness is highest when $\mathbf{g}_c = 3$ and decreasing asymptotically for $\mathbf{g}_c = [4, 5]$, both for simultaneous and subsequent sampling cases. The $\mathbf{g}_c$ to be selected depends on the desired reconstruction quality and the cost of the sensing configurations, which is critical, for example, for the robotic applications with limited battery life. With the strongest improvement $\mathbf{g}_c = 3$ provides arguably a good reconstruction quality. Similarly, the error reduction in JS-div is also at the highest when $\mathbf{g}_c = 3$. The best reconstructions for one test case of Fig. 2(b) based on Nearness are visualized in Fig. 4. Practically speaking, $\mathbf{g}_c = 3$ returns a cost effective solution quality for the minimum number of sensing configurations.

Evaluation of the cross angles: The results for the reconstruction error against the pair-wise cross angles between the sensing configurations are shown in Fig. 5: Fig. 5(a)-5(b) are for Nearness, and Fig. 5(c)-5(d) are for JS-div. Since the scale of the reconstruction error can be different for each test case,

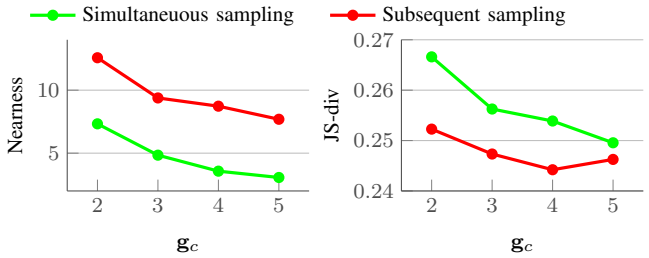

Fig. 3: The reconstruction quality for Nearness and JS-div.

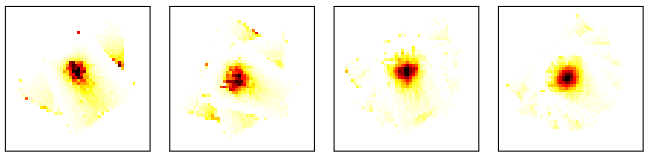

(a) $\mathbf{g}_c = 2$ (b) $\mathbf{g}_c = 3$ (c) $\mathbf{g}_c = 4$ (d) $\mathbf{g}_c = 5$

Fig. 4: The best reconstructions for the test case in Fig. 2(b).

the corresponding errors are first normalized and then averaged over all the cases.

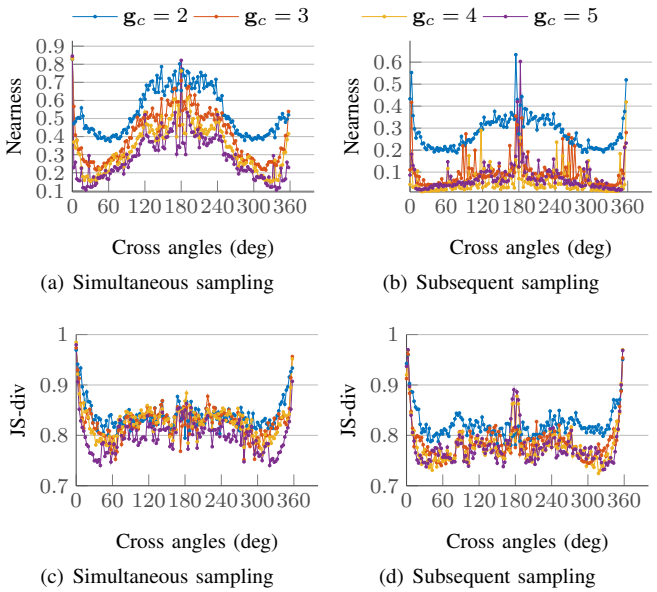

(a) Simultaneous sampling (b) Subsequent sampling

(c) Simultaneous sampling (d) Subsequent sampling

Fig. 5: The results for the cross angles between the configurations. The errors are normalized for each test case and then the average results are plotted for each $\mathbf{g}_c$ against the cross angles.

Given the geometrical layout of the real-world environments, it is not always possible to select the configurations at an exact cross angle. Instead, a range of preferred cross angles that can provide a similarly high quality of reconstruction is desired. We thus selected the 20 best reconstructions from our evaluation and identified the corresponding range of best cross angles. Fig. 5 shows the four different results for the cross angles – for the types of errors and the sampling. The range of cross angles for the best 20 reconstructions is considered from each result. Moreover, the results of the cross angles in the second half of the circle are nearly symmetric to the first half, so all the angles are wrapped within the half circle. Therefore, a total of 8 different ranges of cross angles are to be considered for each $\mathbf{g}_c$. The final range of best cross angle is thus the intersection of all the eight ranges from the graphs. To summarize, the range of best cross angles are $[42.5°, 75°]$ for $\mathbf{g}_c = 2$, $[52.5°, 55°]$ for $\mathbf{g}_c = 3$, and $[37.5°, 40°]$ for both $\mathbf{g}_c = 4$ and $\mathbf{g}_c = 5$. Based on the above experimental evaluation, we can conclude that, for an effective and truthful reconstruction, $\mathbf{g}_c = 3$ with pair-wise cross angles in the range of $[52.5°, 55°]$ is preferred. $\mathbf{g}_c = 2$ should be considered in case placement of 3 configurations is not possible due to obstacles in the environment.

IV. Discussion

In RAGT, the sensing geometries are of high importance for the reconstruction quality. Intuitively, a high number of configurations can yield a better reconstruction. As our paper shows, it is important to select a suitable sensing geometry and we present criteria for this selection. This is due to the fact that the cross angles between the optical paths of the configurations play a role in the reconstruction quality. We investigated sensing geometries of different configurations and their cross angles using a realistic gas dispersion simulator. We then compared reconstructions for 19 realistic environments of different wind speeds and obstacles. The investigations are based on the global reconstruction error and divergence of the PDFs of the gas concentrations. The results suggest that 3 sensing configurations with pairwise cross angles in the range of $[52.5°, 55°]$ produces the best results. As a possible extension of our work, sensing geometries with different sensing parameters can be used to understand why certain geometries produce better reconstructions than the others.

Application in Sensor Planning: A sensor planning framework for RAGT generates an exploration plan that provides a sorted list of sensing configurations to build a gas distribution map of the environment. The evaluation results presented in this paper are useful to maximize the reconstruction quality by placing the desired number of configurations with preferred cross angles around the areas of interest [3]. The concluded geometries can thus be adopted as a desired solution for the sensor planning algorithms for RAGT to improve the tomographic reconstruction in realistic and complex environments.

References

[1] V. Hernandez Bennetts, E. Schaffernicht, T. Stoyanov, A. J. Lilienthal, and M. Trincavelli, "Robot Assisted Gas Tomography - Localizing Methane Leaks in Outdoor Environments," in *IEEE International Conference on Robotics & Automation (ICRA)*, 2014, pp. 6362–6367.

[2] L. Todd and G. Ramachandran, "Evaluation of Optical Source-Detector Configurations for Tomographic Reconstruction of Chemical Concentrations in Indoor Air," *American Industrial Hygiene Association Journal*, vol. 55, no. 12, pp. 1133–1143, 1994.

[3] M. A. Arain, E. Schaffernicht, V. Hernandez Bennetts, and A. J. Lilienthal, "The Right Direction to Smell: Efficient Sensor Planning Strategies for Robot Assisted Gas Tomography," in *IEEE International Conference on Robotics & Automation (ICRA)*, 2016, pp. 4275–4281.

[4] V. Hernandez Bennetts, A. J. Lilienthal, E. Schaffernicht, S. Ferrari, and J. Albertson, "Integrated simulation of gas dispersion and mobile sensing systems," in *RSS Workshop on R4SIM*, 2015.

[5] J. Lin, "Divergence measures based on the shannon entropy," *IEEE Transactions on Information Theory*, vol. 37, no. 1, pp. 145–151, 1991.